



Contents lists available at ScienceDirect

Journal of Organometallic Chemistry

journal homepage: www.elsevier.com/locate/jorganchem

Note

Luminescence and spectroscopic studies of organometallic rhodium and rhenium multichromophore systems carrying polypyridyl acceptor sites and phenylethynyl antenna subunits

Kerstin Oppelt^a, Daniel. A.M. Egbe^b, Uwe Monkowius^a, Manuela List^c, Manfred Zabel^d, Niyazi S. Sariciftci^b, Günther Knör^{a,*}

^a Institut für Anorganische Chemie, Johannes Kepler Universität Linz (JKU), A-4040 Linz, Austria

^b Institut für Physikalische Chemie, Johannes Kepler Universität Linz (JKU), A-4040 Linz, Austria

^c Institut für Chemische Technologie Organischer Stoffe, Johannes Kepler Universität Linz (JKU), A-4040 Linz, Austria

^d Zentrale Analytik, Röntgenstrukturanalyse, Universität Regensburg, 93053 Regensburg, Germany

ARTICLE INFO

Article history:

Received 20 August 2010

Accepted 9 November 2010

Keywords:

Electronic spectra

Luminescence

Rhenium complexes

Rhodium complexes

Multichromophore systems

Phenyleneethynylene ligands

ABSTRACT

The synthesis, structure, photophysics, and spectroscopic characterization of two novel organometallic rhodium and rhenium multichromophore photosensitizers carrying a central 2,2'-bipyridyl acceptor moiety are reported. Due to the presence of rigid phenylethynyl substituents in their 5,5'-position acting as intramolecular antenna groups, these compounds display perturbed excited state properties and a modified luminescence behaviour compared to the unsubstituted parent systems. The rhodium derivative is characterized by a weak blue–green intraligand (IL) phosphorescence occurring only at low temperatures. In the rhenium complex both a blue–green ligand-based luminescence and a red phosphorescence of metal-to-ligand charge transfer (MLCT) origin is observed at room temperature in solution. In rigid 77 K matrix the lowest-lying excited state levels approximate in energy and a structured luminescence band occurs which is ascribed to a ligand phosphorescence with admixed MLCT character.

© 2010 Elsevier B.V. All rights reserved.

1. Introduction

1,2-diimine chelates are a versatile class of π -acceptor ligands, which comprise the frequently studied polypyridyl systems. Investigations of polypyridyl transition metal complexes have led to numerous important applications in solar chemistry, optoelectronics and photocatalysis [1–4]. The by far most comprehensively investigated derivatives are those with a ruthenium 1,2-diimine structural motif [5]. One of the more recent synthetic strategies to control the excited state lifetimes and energies of ruthenium polypyridyl compounds is the attachment of weakly-coupled organic chromophore subunits in their ligand periphery [6,7]. This kind of chemical modification leads to the introduction of additional low-lying excited state levels, which can drastically influence the luminescence characteristics and photochemical behaviour of such multichromophore systems compared to the corresponding unsubstituted coordination compounds. In the present work we explored this possibility and studied the effects of symmetrically

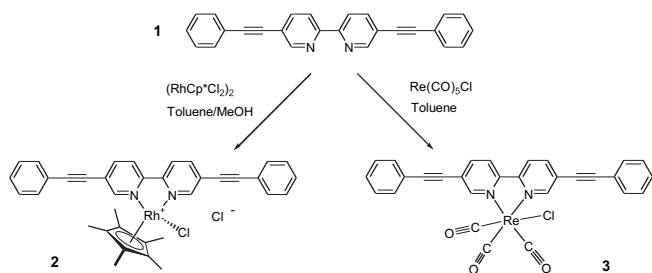
attached phenylethynyl units on the photophysical properties of two novel organometallic rhenium and rhodium polypyridyl complexes. The metallation routes and structural formulae of these compounds are summarized in Scheme 1.

The corresponding unsubstituted 2,2'-bipyridyl complexes with low-valent rhenium carbonyl and rhodium cyclopentadienyl moieties are widely investigated organometallic compounds. While rhenium(I) tricarbonyl polypyridyl complexes in general offer interesting photophysical properties due to their prominent metal-to-ligand charge transfer (MLCT) excited states [8,9], they have also attracted considerable interest in the context of photocatalytic carbon dioxide reduction [10–12]. The reduced rhodium cyclopentadienyl systems on the other hand are versatile reagents for the acceleration of selective hydride transfer processes [13–15]. Especially the complex [Cp*Rh(2,2'-bipyridyl)Cl]Cl and some of its derivatives were extensively used for mediating the chemical or electrocatalytic regeneration of reduced nicotinamide cofactors required for enzymatic substrate transformations [16,17].

Compounds with structural motifs such as **1** are key-components for the design of conjugated fluorescent polymers, which are important materials with many applications in electronic and photonic devices [18]. Therefore, the photophysical properties of the

* Corresponding author.

E-mail address: guenther.knoer@jku.at (G. Knör).



Scheme 1. Reaction of 5,5'-bisphenylethynyl-2,2'-bipyridine (**1**) to form the rhodium Cp* complex (**2**) and the rhenium tricarbonyl chloride complex (**3**).

ligand system 5,5'-bisphenylethynyl-2,2'-bipyridine (**1**) [19,20] and of the closely related 4,4'-substituted phenyleneethynylene based bipyridine derivatives [21] have already been characterized to some extent. In this context, the novel compounds **2** and **3** reported here can be considered as useful monomeric model species for studying the intrinsic spectroscopic features of organometallic poly-arylene-ethynylene polymers containing functional rhenium or rhodium sites. In the case of the rhenium(I) system, a similar modification of the bipyridyl core with covalently attached ethynylated aryl substituents in the 5,5'-position of the ligand has been carried out before in Kirk Schanze's group [22,23], where two additional alkoxy-groups were introduced to influence the solubility and photophysical properties of the compounds. To the best of our knowledge, no such systems have been described before for rhodium functionalized derivatives. The synthesis, structural characterization, electronic spectra and luminescence properties of **2** and **3** are reported here and briefly discussed in terms of potential applications in optoelectronics and photocatalysis.

2. Results and discussion

2.1. Synthesis and structures

The multichromophoric diimine ligand 5,5'-bisphenylethynyl-2,2'-bipyridine (**1**) was obtained from 2,2'-bipyridine according to published routes via the formation of 5,5'-dibromo-2,2'-bipyridine [24], followed by Pd-catalyzed Sonogashira coupling of the dibromo-compound with phenylacetylene [25,26]. Metallation of **1** to form the rhodium half sandwich complex $[\text{Cp}^*\text{Rh}(5,5'\text{-bisphenylethynyl-2,2'-bipyridyl})\text{Cl}]\text{Cl}$ (**2**) was carried out with $[\text{Cp}^*\text{RhCl}_2]_2$ as the metal source in a modified literature procedure [13], using additional toluene to account for the low solubility of the free ligand in methanol. The synthesis of the rhenium complex **3** was readily achieved by using $\text{Re}(\text{CO})_5\text{Cl}$ following well-established metallation routes described in the literature [27–29].

Single crystals of **3** suitable for structure determination by X-ray diffraction were obtained from acetonitrile/diethylether. The compound crystallizes in the triclinic space group P-1 with $Z = 2$ molecules in the unit cell. Although the complexes in crystals of **3** show no crystallographically imposed symmetry, they closely approach a mirror symmetry with the mirror plane including Re1, C11 and C28. The Re(I) atom exists in a distorted octahedral environment defined by a *fac* arrangement of the three carbonyl groups, the chloride atom and the two nitrogen atoms of the bpy ligand (Fig. 1). The distortion from the octahedral symmetry essentially arises from the steric demands of the bpy ligand. The bite angle of the bpy [$\angle(\text{N1}-\text{Re1}-\text{N2})$ 74.9(1)°] is very similar to the bite angles of several complexes of the type $[(s\text{-bpy})\text{Re}(\text{I})(\text{CO})_3\text{X}]$ ($X = \text{anionic or neutral ligand}$) containing a substituted bpy ligand [$\angle(\text{N}-\text{Re}-\text{N})$ ca. 74°] [30]. The bpy moiety is almost perfectly planar [$\angle(\text{N1}-\text{C1}-\text{C2}-\text{N2})$ 0.3(5)°] and the phenyl rings are only slightly rotated out of the bpy plane [$\angle(\text{C10}-\text{C9}-\text{C4}-\text{C5})$ 14.7° and $\angle(\text{C22}-\text{C21}-\text{C17}-\text{C16})$ 1.3°].

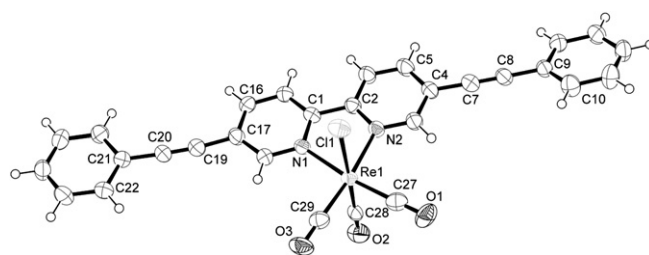


Fig. 1. Molecular structure of complex **3** (50% probability ellipsoids shown). Selected bond lengths [Å] and angles [°]: Re1–N1 2.178(3), Re1–N2 2.177(3), Re1–C11 2.468(1), Re1–C27 1.925(4), Re1–C28 1.949(4), Re1–C29 1.928(5), C11–Re1–N1 83.42(8), C11–Re1–C27 95.55(14), C11–Re1–C28 175.99(12), N1–Re1–N2 74.91(11), C27–Re1–C28 87.91(18), C27–Re1–C29 88.14(19), Re1–N1–C1 117.0(2), C4–C7–C8 178.9(5), C7–C8–C9 179.1(4), C19–C20–C21 177.4(4), C17–C19–C20 174.7(4).

The aromatic rings of the ligands are associated via π -interactions with closest contacts of ca. 3.4 Å (Fig. 2). The characteristic bond lengths and angles are normal and are similar to previously reported values in analogous bpy complexes [30].

Crystals of **2** were obtained from dichloromethane/*n*-pentane. The compound crystallizes in the monoclinic space group P2₁/n ($Z = 4$). The quality of the structural data is less accurate because the crystals contain an unspecific number and type of solvent molecules, which also obstruct the reliable location of the chloride counterion. The rhodium atom displays the three-legged 'piano stool' geometry. It is coordinated by one $\eta^5\text{-Cp}^*$ group, one chloride ligand and two nitrogen atoms of the bpy ligand. The Cp* ligand is almost symmetrically bound to the Rh atom with a mean Rh–C distance of 2.15 ± 0.02 Å.

The bite angle of the bpy [$\angle(\text{N1}-\text{Rh1}-\text{N2})$ 76.3(2)°] as well as the bond distances Rh1–N1, 2.11(1), Rh1–N2, 2.12(1), and Rh1–C11, 2.394(2) Å are close to values of related $[(s\text{-bpy})\text{Rh}(\text{III})\text{Cp}^*\text{Cl}]^+$ complex cations [31]. Contrary to **3** the bpy ligand deviates slightly from planarity [$\angle(\text{N1}-\text{C1}-\text{C2}-\text{N2})$ 4.5(9)°], therefore the metal-lacyclic moiety containing Rh1, N1, C1, C2, and N2 is also not planar but adopts an envelope conformation with the Rh atom lying outside of the NCCN plane. The phenyl groups are considerably rotated against the pyridyl rings of the bpy ligand [$\angle(\text{C5}-\text{C4}-\text{C9}-\text{C14})$ 17.8° and $\angle(\text{C16}-\text{C17}-\text{C21}-\text{C26})$ 25.9°]. Some π - π contacts are present between the bpy ligands with shortest distances of ca. 3.6 Å (Fig. 3).

2.2. Electronic spectra and luminescence

At room temperature in solution the ligand 5,5'-bisphenylethynyl-2,2'-bipyridine (**1**) displays two broad absorption features in

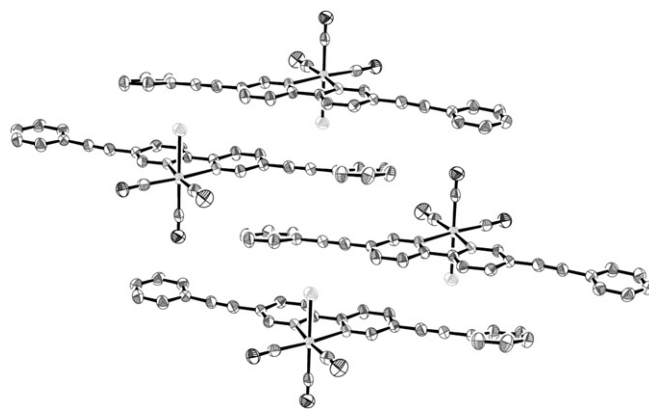


Fig. 2. Excerpt from a cell plot of the crystalline phase of compound **3** depicting the association of the complexes via π - π -interaction. H atoms are omitted for clarity.

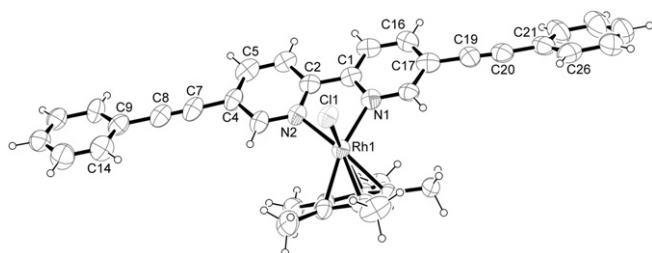


Fig. 3. Molecular structure of the complex cation in crystals of **2** (30% probability ellipsoids shown). Selected bond lengths [Å] and angles [°]: Rh1–N1 2.11(1), Rh1–N2 2.12(1), Rh1–C1 2.394(2), Rh1–C27 2.17(1), Rh1–C28 2.15(1), Rh1–C29 2.14(1), Rh1–C30 2.15(1), Rh1–C31 2.16(1), N1–Rh1–N2 76.3(2), C1–Rh1–N1 90.1(2), C1–Rh1–N2 88.8(2).

the ultraviolet region, which are dominated by the π – π^* electronic transitions of the 2,2'-bipyridine core and the phenylacetylide moieties (Fig. 4).

In dichloromethane the corresponding band maxima are situated at 281 and 344 nm, which are in good agreement with the published data measured in chloroform [20]. The long-wavelength peak maximum is slightly shifting to the blue with increasing solvent polarity (e.g. $\lambda_{\text{max}} = 339$ nm in ethanol), most probably

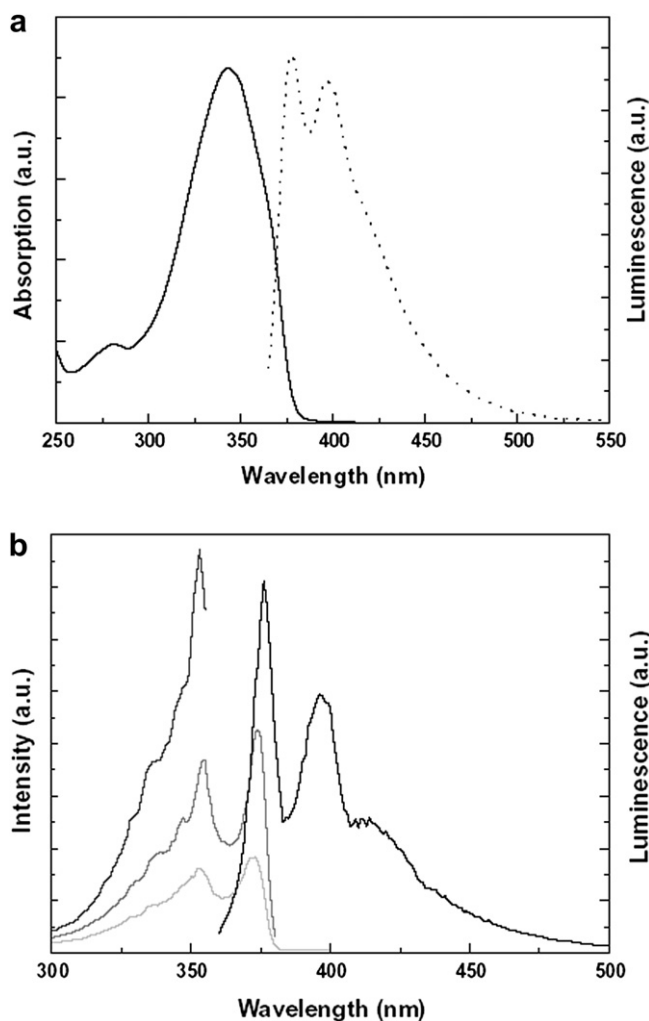


Fig. 4. a) Absorption and emission spectra of the free ligand **1** at room temperature in dichloromethane solution. b) Emission ($\lambda_{\text{exc}} = 340$ nm) and excitation spectra (measured for 376 nm, 397 nm and 420 nm) of the free ligand **1** in 2-methyl-tetrahydrofuran (MTHF) glass at 77 K.

indicating the presence of an additional n – π^* transition covered within the broad envelope of the main absorption band. As shown in Fig. 4, solutions of the free ligand display a blue luminescence [20], which within the well-known limitations of strong pH sensitivity and potential solvent purity effects [1] is assigned to an intraligand (IL) fluorescence involving the conjugated π -electron system of **1**. As expected, the vibronic structure of this emission band is much better resolved and slightly narrowed in the low-temperature luminescence spectra recorded at 77 K in rigid glasses (Fig. 4b).

The corresponding fluorescence excitation spectra recorded for the main peak maxima match the lowest-energy ligand absorption band with a clearly resolved mirror-image peak pattern and a regular spacing of approximately $1400 \pm 50 \text{ cm}^{-1}$ assigned to C=C vibrational modes also present in the infrared spectra of the compound. A rather small Stokes shift of 200 cm^{-1} and an energy of $E_{(0-0)} = 26700 \text{ cm}^{-1}$ (3.31 eV) can be derived for the first excited singlet state of the free ligand under these conditions. No intraligand phosphorescence is observed at 77 K.

The absorption spectra of the complexes **2** and **3** are also dominated by the π – π^* electronic transitions of the free diimine ligand, which are however shifted to longer wavelengths for about 3500 cm^{-1} upon metal coordination (Fig. 5).

In dichloromethane solution the rhodium and the rhenium compounds are characterized by broad absorption maxima at 383 and 389 nm, respectively. Additional weaker UV-bands of intraligand origin are occurring in the 300–320 nm spectral region. These bands display an energetic splitting of approximately 2200 cm^{-1} suggesting a significant coupling to the phenylethynyl C≡C vibrational modes. In the rhodium(III) complex **2** an additional well-resolved peak at 240 nm occurs, which is tentatively assigned to a $\text{Cp}^* \rightarrow \text{Rh}$ ligand-to-metal charge transfer (LMCT) transition similar to other isoelectronic cyclopentadienyl derivatives with a d^6 -configuration [32]. In contrast, the rhenium(I) derivative **3** shows additional $\text{Re} \rightarrow \text{diimine}$ (d – π^*) metal-to-ligand (MLCT) charge transfer absorption bands to the red of the intraligand transitions [27], which in dichloromethane occur in the visible spectral region around 425 and 470 nm (Fig. 5). Furthermore, a relatively weak shoulder is observed at 400 nm, which is assigned to the characteristic $\text{Re} \rightarrow \text{CO}$ MLCT transition present in all metal complexes carrying a rhenium(I) carbonyl moiety [33]. The lowest energy MLCT bands of the rhenium complex show the

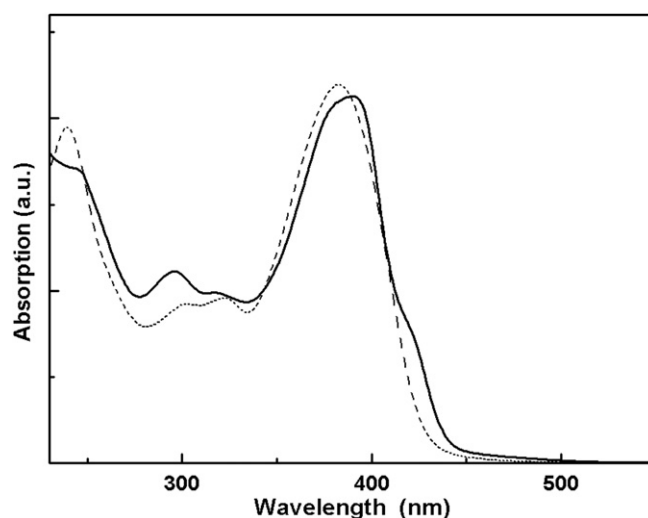


Fig. 5. Electronic absorption spectra of the rhodium (**2**, dotted line) and rhenium (**3**, solid line) complexes in dichloromethane at r.t.

typical negative solvatochromism with a blue shift of the corresponding band maxima in more polar solvents. The charge transfer shoulders in the absorption spectra are therefore less well separated from the strong intraligand (IL) band in acetonitrile solution, where a resulting maximum of 375 nm is observed. The sensitivity of the MLCT bands of compound **3** to solvent polarity effects is in the same range as for the unsubstituted 2,2'-bipyridyl parent compound [27]. Interestingly, the spectra of the rhodium derivative **2** also exhibit some solvent dependency. For example, the broad intraligand band at 383 nm (Fig. 5) is hypsochromically shifted to 373 nm in ethanol and is situated at 372 nm in acetonitrile solution. In contrast to the charge transfer dependent solvatochromism observed for the rhenium system **3**, this behaviour can most probably be ascribed to a ligand exchange process of the chloride ligand of **2** against H₂O under these conditions, which is a typical reaction for similar rhodium complexes [14].

The assignment of the lowest-lying excited states of the compounds **2** and **3** as intraligand (IL) and metal-to-ligand charge transfer (MLCT) type is in agreement with the results obtained from supporting theoretical calculations at the DFT level (Fig. 6). In the rhodium system **2** the frontier orbital transition mainly involves the delocalized π -electron system of the phenylethynyl substituted ligand moiety **1**. In contrast, the highest occupied molecular orbital of the rhenium complex carries a significant metal d-orbital contribution from the Re(CO)₃Cl fragment, which determines the charge transfer character of the lowest excited states in **3**.

The luminescence properties of [Cp**Rh*(5,5'-bisphenylethynyl-2,2'-bipyridyl)Cl]Cl (**2**) and (5,5'-bisphenylethynyl-2,2'-bipyridyl)Re(CO)₃Cl (**3**) were studied both at room temperature in fluid solution and in solid low-temperature matrix at 77 K. In the rhodium system **2**, the strong blue fluorescence of the free diimine ligand (Fig. 4) is completely quenched, and no luminescence could be detected at room temperature in aerated or argon saturated solvents. At low temperature the compound displays a weak and slightly structured luminescence (Fig. 7), which – in agreement with the typical luminescence behaviour of other rhodium polypyridyl complexes – is ascribed to an intraligand (IL) phosphorescence from a $^3\pi-\pi^*$ state to the ground state [34]. Emission maxima and shoulders are occurring with an average spacing of 1450 cm⁻¹ at 431, 460, 493 and around 530 nm, respectively, which is consistent with such an assignment. The corresponding excitation spectrum of this phosphorescence (Fig. 7) is quite similar to the 77 K excitation spectrum obtained for the free ligand fluorescence

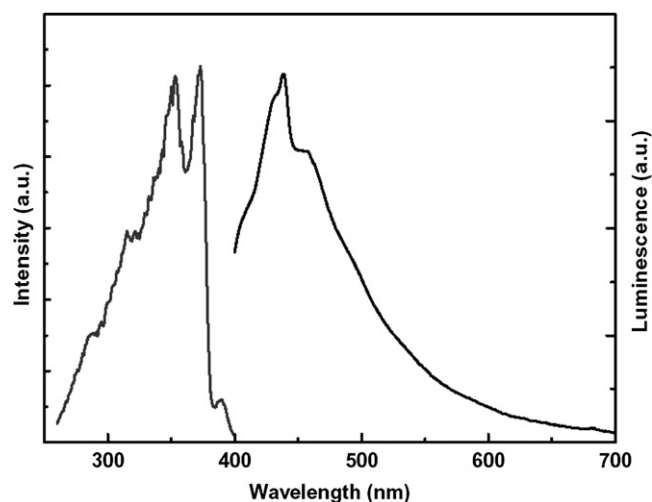


Fig. 7. Emission ($\lambda_{\text{exc}} = 390$ nm) and excitation spectrum of the rhodium Cp* complex **2** in 2-methyltetrahydrofuran glass at 77 K.

(Fig. 4b) and shows a well-resolved vibronic structure with two main maxima at 355 and 374 nm and an additional feature at 390 nm matching the absorption maximum of the compound. A Stokes shift of approximately 3500 cm⁻¹ can be derived for this intraligand phosphorescence.

Usually, the effects of spin-orbit coupling and increasing inter-system crossing rates in the presence of a “heavy” second-row transition element are made responsible for the modified ligand photophysics observed in homoleptic rhodium diimine systems. For other compounds, this simplified picture may sometimes be misleading and recently has even been questioned because of the unexpected observation of apparently fluorescent organometallic rhodium emitters [35]. In this context it is important to note that several other reasons for a more complex photophysical behaviour may exist, which should also be taken into account for an interpretation of the luminescence properties of heteroleptic rhodium (III) diimine complexes such as **2**. Besides low-lying intraligand excited states, the deactivation pathways of such systems may also involve metal-centered (MC) triplet states of ^3d-d origin [36] or may be complicated by ligand-to-ligand charge transfer (LLCT) excited states at rather low energies, which is sometimes the case

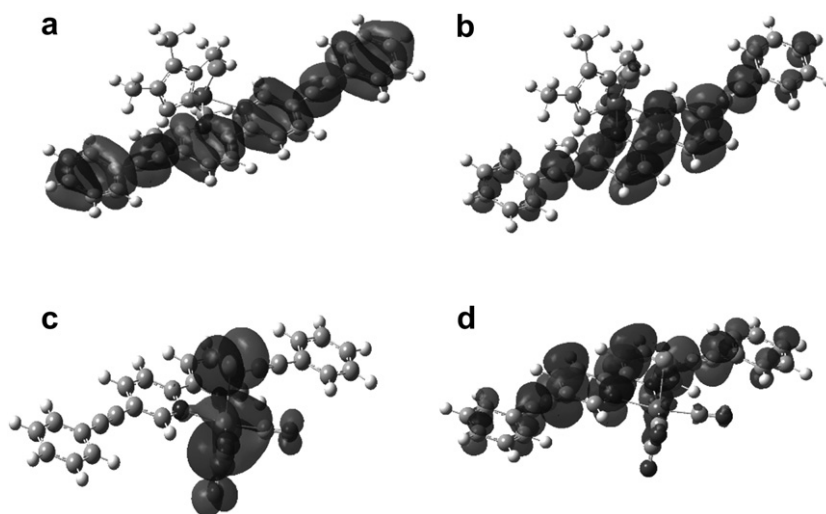


Fig. 6. Frontier orbitals of the rhodium and rhenium derivatives studied in the present work: (a) HOMO and (b) LUMO of the rhodium compound **2**; (c) HOMO and (d) LUMO of rhenium complex **3**.

in the presence of cyclopentadienyl donor ligands [37]. Frequently, the energetic separation of close-lying electronic levels of different orbital parentage is small, which makes these systems very sensitive to minor chemical modifications and may also lead to a pronounced temperature dependency of the photophysical properties. The nature of the lowest excited states of the rhodium complex **2**, however, can be described within the regular framework of intraligand $\pi-\pi^*$ transitions modified by the effects of spin-orbit coupling induced by the coordinated heavy metal ion.

The photophysics of the rhenium complex **3** is dominated by the presence of the reducing rhenium(I) tricarbonyl chloride donor fragment, which leads to a luminescent lowest-energy triplet excited state of the metal-to-ligand charge transfer (MLCT) type [8,9]. The broad $^3\text{MLCT}$ emission of **3** in dichloromethane solution is covering the spectral region of orange and red light with a maximum at around 650 nm and additional shoulders at 590 and 700 nm (Fig. 8). Interestingly, upon UV-light excitation at the absorption peak maximum of **3**, the compound also shows an additional structured blue–green intraligand emission with maxima at 443 and 465 nm, which obviously is not completely quenched by the lower-lying MLCT states (Fig. 8). This feature is not observed in the unsubstituted parent compound (2,2'-bipyridyl)Re(CO)₃Cl and therefore is ascribed to the presence of the additional phenylethyne units in 5,5'-position of the diimine ligand system **1**. A comparable dual luminescence behaviour has also been reported for similar multichromophore systems investigated by Schanze and coworkers [23]. We have carried out careful control experiments to exclude contaminations of luminescent free ligand in our samples. The analysis of the corresponding excitation spectra also indicates the authenticity of this additional IL luminescence at higher energies. Argon saturation of the samples only leads to a moderate increase of both the intraligand and the MLCT luminescence bands without changing the ratio of both emissions.

When the luminescence of the compound is recorded at 77 K in rigid MTHF glass, the short-wavelength intraligand contribution completely disappears and only one structured emission band with maxima at 567, 619, 675 and a shoulder at 753 nm is observed (Fig. 9). The excitation spectrum of this luminescence shows a peak at 317 nm, two main maxima at 373 and 395 nm, and an additional contribution from the weaker absorption features in the MLCT band region above 400 nm (Figs. 5 and 9). Both excitation and emission

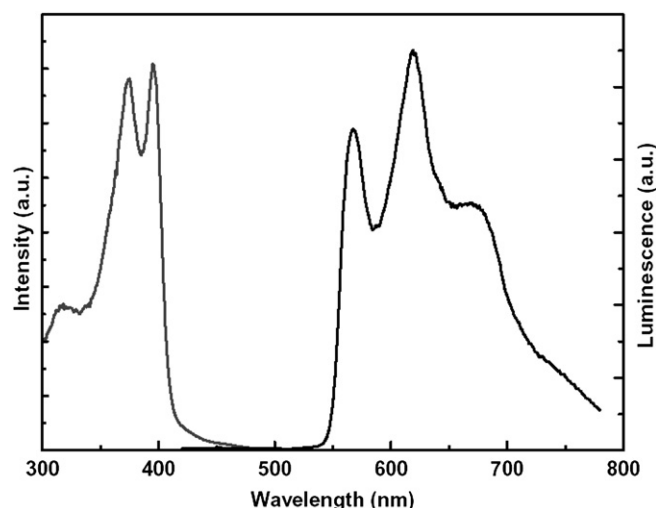


Fig. 9. Emission ($\lambda_{\text{exc}} = 340$ nm) and excitation spectrum of the rhenium complex **3** in 2-methyltetrahydrofuran glass at 77 K.

bands display a pronounced vibronic pattern with an average spacing of 1450 cm^{-1} consistent with a significant intraligand character of the corresponding excited states. On the other hand, the observed Stokes shift of the emission (9200 cm^{-1}) is much larger than in the rhodium case (Fig. 7), thus indicating also a considerable amount of charge transfer in the electronic transition. At 77 K the corresponding excited state is therefore best described as considerably mixed IL ($^3\pi-\pi$) and MLCT ($^3\text{d}-\pi^*$) type.

This interesting temperature and medium dependent switch in the luminescence behaviour of the rhenium multichromophore compound **3** can be interpreted in terms of the different excited state properties of typical IL versus MLCT chromophore systems. Compounds with intraligand excited states involving an electron redistribution within a larger delocalized π -electron system usually show only minor structural variations upon light absorption. As a consequence, the radiative rates are frequently rather high and there is only a moderate perturbation of the corresponding emission spectra upon solvent variation or inclusion into a rigid matrix such as a low temperature solvent glass. On the other hand, charge transfer excitation may lead to significant changes in the dipole moment and geometry of an excited state species. In the case of rhenium diimine complexes, the MLCT emission maxima typically undergo hypsochromic shifts and the corresponding excited state energy rises as the medium rigidity increases (luminescence rigidochromic effect [38]). This well-known behaviour may help to tentatively interpret the unusual photophysics observed for (5,5'-bisphenylethyne-2,2'-bipyridyl)Re(CO)₃Cl (**3**). In contrast to the situation in unsubstituted rhenium diimine systems, the presence of phenylethyne subunits in **3** lowers the energy gap between IL and MLCT excited state levels. Therefore, in dichloromethane the corresponding absorption bands nearly overlap (Fig. 5). Upon excitation at room temperature in solution, an efficient intersystem crossing occurs and the broad orange–red MLCT ($^3\text{d}-\pi^*$) phosphorescence band is observed. However, the high radiative rate of the intraligand states also populated with 390 nm light offers an alternative excited state deactivation pathway and to some extent an additional IL emission is also possible. When other solvents such as MTHF are used, the effect of negative solvatochromism shifts the MLCT levels to higher energies and the situation of nearly degenerate states of different orbital parentage becomes even more pronounced. The corresponding thermal equilibrium distribution between close-lying IL and MLCT levels is suggested to be gradually frozen out at lower temperatures. When a rigid glassy matrix is

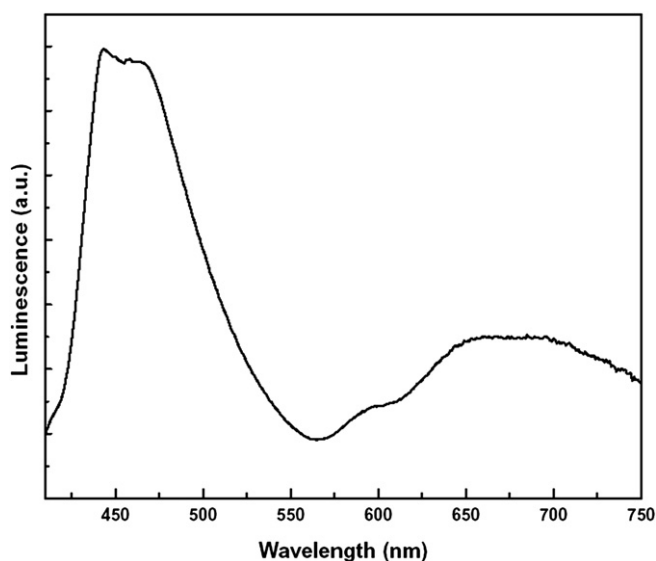


Fig. 8. Emission spectrum ($\lambda_{\text{exc}} = 390$ nm) of the rhenium tricarbonyl chloride complex **3** in dichloromethane solution at room temperature.

formed at 77 K, the rigidochromic effect leads to a further destabilization of the charge transfer levels and the energies of the IL and MLCT states more or less coincide or even may be inverted. Obviously, for compound **3** only the emission resulting from the lowest-lying excited triplet state is possible under these conditions and the short-wavelength luminescence component disappears. As the experimental data suggest (Fig. 9), also the nature of this emissive excited state changes to an intermediate IL/MLCT type while a more extensive mixing in the excited state configurations occurs. A similar situation of a temperature dependent emission re-ordering in rhenium diimine complexes with close-lying IL and MLCT states has been reported before [39].

As a conclusion, the attachment of phenylethynyl substituents to the 5,5'-position of bipyridyl ligands is a simple and straightforward method to modify the excited state properties of the corresponding metal complexes. Such a substitution may influence the degree of orbital mixing and can be used to control the degeneracy of close-lying excited state levels of different orbital parentage. This synthetic strategy may therefore lead to completely new reactivity and luminescence characteristics with potential implications for optoelectronic and photocatalytic systems.

3. Experimental

3.1. Materials and methods

3.1.1. General methods

Unless otherwise stated, all chemicals and solvents were purchased in reagent or technical grade quality and directly used as received. Thin layer chromatography (silica gel 60, 0.2 mm, GF₂₅₄) was performed with the same solvents as used for column chromatography. New compounds were characterized by elemental analysis, IR-, NMR- and ESI mass spectroscopy. ¹H and ¹³C NMR spectra were obtained with a Bruker Avance DPX 200 NMR-Spectrometer. IR measurements were performed with a Shimadzu IRAffinity-1 Fourier Transform Infrared Spectrometer equipped with a Specac Golden Gate diamond ATR system. Absorption Measurements were performed in 1 cm quartz glass cuvettes with a Cary 300 Bio UV–Visible spectrophotometer or with a Jasco V-670 spectrophotometer. Luminescence measurements were performed with a Horiba Yobin Ivon Fluorolog-3 spectrofluorometer. For room temperature experiments the solution was purged with argon before measurement, if not otherwise stated.

3.1.2. Crystal structure determination

Diffraction data for crystals of the compounds **2** and **3** were collected with an Oxford Diffraction Gemini Ultra CCD diffractometer with multilayer optics and Cu-K α radiation ($\lambda = 1.5418 \text{ \AA}$). Further crystallographic and refinement data can be found in Table S1 (see Supplementary Material). The structures were solved by direct methods (SIR-97) [40] and refined by full-matrix least-squares on F² (SHELXL-97) [41]. The H atoms were calculated geometrically and a riding model was applied during the refinement process.

3.1.3. Computational details

The Gaussian03 program was used in the calculations [42]. Initial coordinates were taken from the corresponding X-ray molecular structure. All quantum-chemical calculations were carried out using a density functional theory (DFT) based method with the hybrid B3LYP [43] functional. The 6-31G(d',p') basis set [44] was used through the calculations, whereas for the complexed metal a LanL2DZ basis set [45] was applied. The obtained geometries were verified to correspond to a real minimum by establishing an absence of imaginary IR frequencies.

3.2. Synthetic procedures

3.2.1. 5,5'-Bisphenylethynyl-2,2'-bipyridine (**1**)

The free ligand **1** was synthesized according to published routes [24–26] starting from 5,5'-dibromo-2,2'-bipyridine. The dibromo-compound was treated for 3 h with an excess of phenylacetylene in the presence of 1 mol-% Pd(PPh₃), 4.2 mol-% of CuI and triethylamine in THF. After chromatographic separation with dichloromethane/ethylacetate (4:1) the crude 5,5'-bis(phenylethynyl)-2,2'-bipyridine was obtained. Further purification was achieved by repeated precipitation of **1** from a THF-solution by the addition of methanol.

R_f = 0.77 (SiO₂, CH₂Cl₂/ethyl acetate 4:1); **¹H NMR** (200 MHz, CDCl₃) δ 8.82 (br-s, 2H, bpy-H6,6'); 8.45 (d, 2H, ³J_{HH} = 8.0 Hz, bpy-H3,3'); 7.95 (dd, 2H, ³J_{HH} = 8.2 Hz, ⁴J_{HH} = 2.1 Hz; bpy-H4,4'); 7.58 (m, 4H, phen-H2,2',6,6'); 7.39 (m, 6H, phen-H3,3',4,4',5,5'); **FT-IR** (ATR): ν/cm^{-1} : 3049 (w, Aryl-H), 2962 (w, Aryl-H), 2921 (w), 1967 (w), 1585 (m), 1569 (w), 1559 (w), 1529 (m), 1507 (w), 1489 (m), 1457 (m), 1439 (m), 1364 (m), 1260 (m), 1231 (m), 1177 (w), 1154 (w), 1127 (w), 1088 (w), 1069 (w), 1022 (m), 967 (w), 931 (m), 915 (m), 845 (s), 798 (s), 758 (s), 750 (s), 738 (s), 714 (m), 689 (s), 670 (m), 650 (s), 622 (w), 552 (w), 539 (m), 515 (s).

3.2.2. [Cp*Rh(5,5'-bisphenylethynyl-2,2'-bipyridyl)Cl]Cl (**2**)

The rhodium complex **2** was synthesized from **1** and [Cp*RhCl₂]₂ according to a modified literature method [13]. In contrast to the published procedure, a mixture of methanol and toluene was used, to improve the solubility of the free ligand. The product was precipitated with anhydrous diethyl ether. After filtration, a part of the crude yellow product was recrystallized from dichloromethane/pentane. Yield: 77%.

¹H NMR (200 MHz, CDCl₃) δ 9.37 (br-d, 2H, ³J_{HH} = 7.0 Hz; bpy-H3,3') 8.73 (s, 2H; bpy-H6,6'); 8.33 (br-d, 2H, ³J_{HH} = 6.7 Hz; bpy-H4,4'); 7.61 (m, 4H, phen-H2,6,2',6'); 7.44 (m, 6H, phen-H3,4,5,3',4',5') 1.77 (s, 15H, Cp*); **¹³C NMR** (200 MHz, CDCl₃, apt) δ 151.6, 142.4, 131.5, 129.4, 128.1, 126.0, 96.6 (quaternary C (Cp*)), 8.7 (CH₃-Cp*); no further quaternary carbons detected. **¹H–¹³C NMR** (200 MHz, CDCl₃, HSQC) δ (H)– δ (C) 9.37–125.98 (bpy-H3,3') 8.83–152.2 (bpy-H6,6') 8.39–143 (bpy-H4,4') 7.68–131.9 (phen-H2,2'-C2, 2') 7.45–128.3 (phen-H3,4,5,3',4',5'-C3,4,5,3',4',5') 1.84–7.4 (CH₃-Cp*). **FT-IR** (ATR): ν/cm^{-1} : 3335 (s, O–H), 3050–2850 (m, Alkyl-H), 2217 (s), 1755 (s), 1650 (w), 1597 (w), 1560 (w), 1494 (s), 1460 (m), 1441 (m), 1378 (s), 1281 (s), 1070 (m), 1047 (w), 1018 (m), 927 (m), 865 (w), 846 (m), 797 (w), 764 (s), 724 (m), 694 (s), 520 (w). **Elemental analysis** Calc. for C₃₆H₃₁N₂RhCl₂ × 3H₂O (*M* = 719.50 mol l⁻¹) C 60.10 H 5.18 N 3.89; Found: C 57.49 H 4.73 N 3.79. **Mass spectrum** (ESI, CHCl₃: i-propanol = 7:3) Calculated: C₃₆H₃₁N₂RhCl⁺ *m/z* (%): 629.07 (100) M⁺.

3.2.3. fac-(5,5'-Bisphenylethynyl-2,2'-bipyridyl)Re(CO)₃Cl (**3**)

The rhenium complex **3** was synthesized according to standard procedures [27–29]. In a typical experiment, a suspension of 52 mg (0.14 mmol) 5,5'-bisphenylethynyl-2,2'-bipyridine, **1**, and 51 mg (0.14 mmol) Re(CO)₅Cl in 20 ml of absolute toluene were refluxed under nitrogen atmosphere for 3 h. Within 10 min, the solution became orange. After cooling the resulting precipitate was separated from the solvent by filtration under N₂ to yield an orange solution. Upon cooling the product crystallizes as a yellow powder, which was washed with 3 ml of toluene and dried under vacuum. The complex was purified by recrystallization from acetonitrile/diethylether.

¹H NMR (200 MHz, CD₃CN) δ 9.1 (d, 2H, ⁴J_{HH} = 1.33 Hz; bpy-H6,6'); 8.47 (d, 2H, ³J_{HH} = 8.6 Hz; bpy-H3,3') 8.35 (dd, 2H, ³J_{HH} = 8.5 Hz, ⁴J_{HH} = 1.8 Hz; bpy-H4,4') 7.65 (m, 4H, phen-H2,2',6,6') 7.45 (m, 6H, phen-H3,3',4,4',5,5'). **¹³C NMR** (200 MHz, CD₃CN, apt) δ 187.1 (quaternary C), 182.4 (quaternary C), 156.8, 154.1 (quaternary C), 142.1, 131.4, 129.7, 128.5, 124.0, no further quaternary carbons

detected. **FT-IR** (ATR): ν/cm^{-1} : 3745 (m), 3150–3050 (w, Ar-H), 2320 (w, CO₂), 2221 (w, alkyne), 2187 (w, alkyne), 2119 (w, alkyne), 2010 (s, CO), 1960 (m, CO), 1887 (s, CO), 1649 (w), 1562 (w), 1465 (w), 1371 (w), 1242 (w), 1117 (w), 1066 (w), 1029 (w), 919 (w), 839 (w), 756 (w), 686 (w), 630 (w), 577 (w).

Acknowledgments

Financial support by the Austrian Science Fund (FWF project P21045: “Bio-inspired Multielectron Transfer Photosensitizers”) and the Solar Fuel GmbH is gratefully acknowledged.

Appendix A. Supplementary material

CCDC 781171 and 781538 contain the supplementary crystallographic data for **2** and **3**. These data can be obtained free of charge from The Cambridge Crystallographic Data Centre via www.ccdc.cam.ac.uk/data_request/cif. Crystallographic details and the results of the quantum-chemical calculation can be found in the Supporting Information.

Appendix. Supporting information

Supporting information associated with this article can be found, in the online version, at doi:[10.1016/j.jorganchem.2010.11.008](https://doi.org/10.1016/j.jorganchem.2010.11.008).

References

- [1] K. Kalyanasundaram, Photochemistry of Polypyridine and Porphyrin Complexes. Academic Press, London, 1992, p. 92.
- [2] D.M. Roundhill, J.P. Fackler Jr. (Eds.), Optoelectronic Properties of Inorganic Compounds, Plenum Press, New York, 1999.
- [3] H. Yersin (Ed.), Highly Efficient OLEDs with Phosphorescent Materials, Wiley-VCH, Berlin, 2007.
- [4] V. Balzani, S. Campagna (Eds.), Photochemistry and Photophysics of Coordination Compounds I, Top. Curr. Chem., vol. 280, 2007.
- [5] A. Juris, V. Balzani, F. Barigelli, S. Campagna, P. Belsler, A. von Zelewsky, Coord. Chem. Rev. 84 (1988) 85–277.
- [6] E.A. Medlycott, G.S. Hanan, F. Loiseau, S. Campagna, Chem. Eur. J. 13 (2007) 2837–2846.
- [7] S. Ji, W. Wu, W. Wu, P. Song, K. Han, Z. Wang, S. Liu, H. Guo, J. Zhao, J. Mater. Chem. 20 (2010) 1953–1963.
- [8] G.L. Geoffroy, M.S. Wrighton, Organometallic Photochemistry. Academic Press, New York, 1979.
- [9] R.A. Kirgan, B.P. Sullivan, D.P. Rillema, Top. Curr. Chem. 281 (2007) 45–100.
- [10] J. Hawecker, J.-M. Lehn, R. Ziessel, J. Chem. Soc., Chem. Commun. (1983) 536–537.
- [11] A.J. Morris, G.J. Meyer, E. Fujita, Acc. Chem. Res. 42 (2009) 1983–1984.
- [12] H. Takeda, O. Ishitani, Coord. Chem. Rev. 254 (2010) 346–354.
- [13] U. Kölle, S.-S. Kang, P. Infelta, P. Comte, M. Grätzel, Chem. Ber. 122 (1989) 1869–1890.
- [14] F. Hollmann, A. Schmidt, E. Steckhan, Angew. Chem. 113 (2001) 190–192; Angew. Chem. Int. Ed. 40 (2001) (2001) 169–171.
- [15] S.H. Lee, D.H. Nam, C.B. Park, Adv. Synth. Catal. 351 (2009) 2589–2594.
- [16] F. Hollmann, B. Witholt, A. Schmidt, J. Mol. Catal., B Enzym. 19 (2002) 167–176.
- [17] K. Vuorilehto, S. Lütz, C. Wandrey, Bioelectrochemistry 65 (2004) 1–7.
- [18] U.H.F. Bunz, Chem. Rev. 100 (2000) 1605–1644.
- [19] U.-W. Grummt, E. Birckner, M. Al-Higari, D.A.M. Egbe, E. Klemm, J. Fluoresc. 11 (2001) 41–51.
- [20] B. Bussemer, D. Munsel, H. Wünsch, G.J. Mohr, U.-W. Grummt, J. Phys. Chem. B 111 (2007) 8–15.
- [21] P.V. James, K. Yoosaf, J. Kumar, K.G. Thomas, A. Listorti, G. Accorsi, N. Armaroli, Photochem. Photobiol. Sci. 8 (2009) 1432–1440.
- [22] K.D. Ley, C.E. Whittle, M.D. Bartberger, K.S. Schanze, J. Am. Chem. Soc. 119 (1997) 3423–3424.
- [23] Y. Liu, Y. Li, K.S. Schanze, J. Photochem. Photobiol. C Photochem. Rev. 3 (2002) 1–23.
- [24] F.M. Romero, R. Ziessel, Tetrahedron Lett. 36 (1995) 6471–6474.
- [25] K. Sanechika, T. Yamamoto, A. Yamamoto, Bull. Chem. Soc. Jpn. 57 (1984) 752–755.
- [26] D.A.M. Egbe, E. Klemm, Macromol. Chem. Phys. 199 (1988) 2683–2688.
- [27] G. Knör, M. Leirer, A. Vogler, J. Organomet. Chem. 610 (2000) 16–19.
- [28] U. Monkowius, S. Ritter, B. König, M. Zabel, H. Yersin, Eur. J. Inorg. Chem. 29 (2007) 4597–4606.
- [29] U. Monkowius, Y.N. Svartsov, T. Fischer, M. Zabel, H. Yersin, Inorg. Chem. Commun. 10 (2007) 1473–1477.
- [30] S. Trammell, P.A. Goodson, B.P. Sullivan, Inorg. Chem. 35 (1996) 1421–1422; P.A. Anderson, F.R. Keene, E. Horn, R.T. Tiekink, Appl. Organomet. Chem. 4 (1990) 523–533; V.W.W. Yam, V.C.Y. Lau, K.-K. Cheung, Organometallics 14 (1995) 2749–2753; O.O. Gerlits, P. Coppens, Acta Crystallogr. Sect. E 57 (2001) m164.
- [31] H. Aneetha, P.S. Zacharias, B. Srinivas, G.H. Lee, Y. Wang, Polyhedron 18 (1999) 299–307; M.A. Scharwitz, I. Ott, Y. Geldmacher, R. Gust, W.S. Sheldrick, J. Organomet. Chem. 693 (2008) 2299–2309; L. Daddi, H. Elias, U. Frey, A. Hörnig, U. Kölle, A.E. Merbach, H. Paulus, J.S. Schneider, Inorg. Chem. 34 (1995) 306–315.
- [32] V. Jakubek, A.J. Lees, Inorg. Chem. 22 (2004) 6869–6871.
- [33] A. Včiek Jr., Coord. Chem. Rev. 230 (2002) 225–242.
- [34] G.A. Crosby, K.W. Hipps, W.H. Elfring Jr., J. Am. Chem. Soc. 96 (1974) 629–630.
- [35] A. Steffen, M.G. Tay, A.S. Batsanov, J.A.K. Howard, A. Beeby, K.Q. Vuong, X.-Z. Sun, M.W. George, T.B. Marder, Angew. Chem. Int. Ed. 49 (2010) 2349–2353.
- [36] J.A. Brozik, G.A. Crosby, Coord. Chem. Rev. 249 (2005) 1310–1315.
- [37] H. Kunkely, A. Vogler, Eur. J. Inorg. Chem. 12 (1998) 1863–1865.
- [38] A.J. Lees (Ed.), Photophysics of Organometallics, Top. Organomet. Chem., vol. 29, 2010, p. 3.
- [39] M. Leirer, G. Knör, A. Vogler, Inorg. Chim. Acta 288 (1999) 150–153.
- [40] A. Altomare, G. Cascarano, C. Giacovazzo, A. Guagliardi, J. Appl. Crystallogr. 26 (1993) 343–350.
- [41] G.M. Sheldrick, Shelxl-97, Program for Crystal Structure Refinement. University of Göttingen, Germany, 1997.
- [42] M.J. Frisch, G.W. Trucks, H.B. Schlegel, G.E. Scuseria, M.A. Robb, J.R. Cheeseman, J.A. Montgomery Jr., T. Vreven, K.N. Kudin, J.C. Burant, J.M. Millam, S.S. Iyengar, J. Tomasi, V. Barone, B. Mennucci, M. Cossi, G. Scalmani, N. Rega, G.A. Petersson, H. Nakatsuji, M. Hada, M. Ehara, K. Toyota, R. Fukuda, J. Hasegawa, M. Ishida, T. Nakajima, Y. Honda, O. Kitao, H. Nakai, M. Klene, X. Li, J.E. Knox, H.P. Hratchian, J.B. Cross, V. Bakken, C. Adamo, J. Jaramillo, R. Gomperts, R.E. Stratmann, O. Yazyev, A.J. Austin, R. Cammi, C. Pomelli, J.W. Ochterski, P.Y. Ayala, K. Morokuma, G.A. Voth, P. Salvador, J.J. Dannenberg, V.G. Zakrzewski, S. Dapprich, A.D. Daniels, M.C. Strain, O. Farkas, D.K. Malick, A.D. Rabuck, K. Raghavachari, J.B. Foresman, J.V. Ortiz, Q. Cui, A.G. Baboul, S. Clifford, J. Cioslowski, B.B. Stefanov, G. Liu, A. Liashenko, P. Piskorz, I. Komaromi, R.L. Martin, D.J. Fox, T. Keith, M.A. Al-Laham, C.Y. Peng, A. Nanayakkara, M. Challacombe, P.M.W. Gill, B. Johnson, W. Chen, M.W. Wong, C. Gonzalez, J.A. Pople, Gaussian 03, Revision C.02. Gaussian, Inc., Wallingford CT, 2004.
- [43] A.D. Becke, Phys. Rev., A 38 (1988) 3098–3100; C.T. Lee, W.T. Yang, R.G. Parr, Phys. Rev., B 37 (1988) 785–789; A.D. Becke, J. Chem. Phys. 98 (1993) 5648–5652.
- [44] R. Ditchfield, W.J. Hehre, J.A. Pople, J. Chem. Phys. 54 (1971) 724–728; W.J. Hehre, R. Ditchfield, J.A. Pople, J. Chem. Phys. 56 (1972) 2257–2261; V.A. Rassolov, M.A. Ratner, J.A. Pople, P.C. Redfern, L.A. Curtiss, J. Comput. Chem. 22 (2001) 976–984.
- [45] P.J. Hay, W.R. Wadt, J. Chem. Phys. 82 (1985) 270–283; W.R. Wadt, P.J. Hay, J. Chem. Phys. 82 (1985) 284–298; P.J. Hay, W.R. Wadt, J. Chem. Phys. 82 (1985) 299–310.